J. Fluid Mech. (1982), *vol.* 122, *pp.* 187–194
Printed in Great Britain

Weakly interacting internal solitary waves in neighbouring pycnoclines

By A. K. LIU, N. R. PEREIRA† AND D. R. S. KO
Dynamics Technology Inc., 22939 Hawthorne Blvd, Suite 200,
Torrance, California 90505

(Received 9 March 1981 and in revised form 29 January 1982)

Weak coupling between nonlinear internal solitary waves on neighbouring pycnoclines allows resonant energy exchange. The lagging wave increases its energy and speed at the expense of the front-running wave, so that the waves leapfrog about an average position. Analytical estimates for this process agree with the wave-tank experiments described in the companion paper by Weidman & Johnson (1982).

1. Introduction

The region between two fluids of different density (the pycnocline) can support a variety of interesting waves. These so-called internal waves are dispersive, and can be nonlinear even for modest amplitudes. Nonlinear solitary waves have been investigated by Keulegan (1953) and Long (1956), by Benney (1966) and Benjamin (1966) for shallow water, and by Benjamin (1967) and Ono (1975) for deep water. For intermediate depths these waves have been investigated by Kubota, Ko & Dobbs (1978) and Joseph (1977). The solitary waves are generally very stable, and are easily generated from quite arbitrary but large perturbations.

In the ocean there are often at least two pycnoclines fairly close together. Eckart (1961) discussed the linear internal-wave problem for two well-separated pycnoclines, and showed the resonant transfer of energy between waves in each of the two pycnoclines. The energy transfer is also possible between solitary waves, each on its own pycnocline. This situation, shown in figure 1, was treated by Liu, Kubota & Ko (1980). They derived two coupled equations for the evolution of the wave amplitudes of single-mode waves propagating along each pycnocline with nearly equal speeds, and investigated the interaction numerically. After initial transients there appear clearly time-periodic solitary waves, which alternate their relative phase relationship as a result of the oscillation of wave amplitudes: the solitary waves are leapfrogging over each other as they propagate.

The coupling between the upper and lower solitary waves is through the induced pressure fields; therefore the interaction is decreasing with increasing separation distance between the pycnoclines. For large separation distance, the coupling between waves is weak. Then the shape of the solitary waves, which is a reflection of the balance between nonlinearity and dispersion, does not change, but the wave parameters change slowly in time in accordance with the energy conservation law (e.g. Pereira & Redekopp 1980).

† Present address: Maxwell Laboratory, 8835 Baldoa Avenue, San Diego, California 92123.

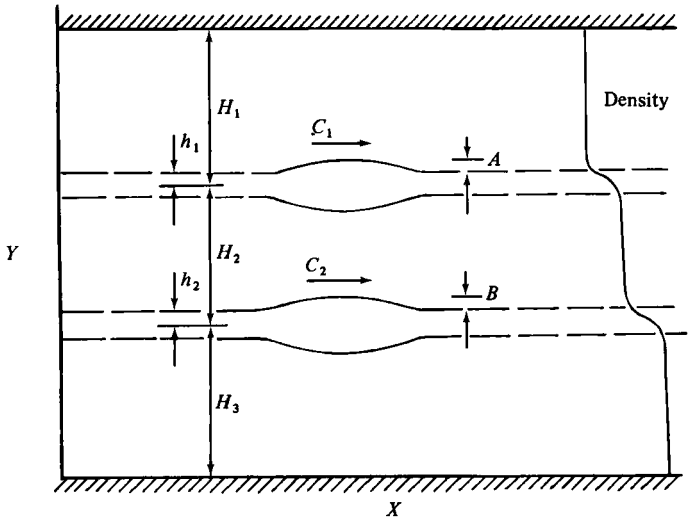

FIGURE 1. Two neighbouring pycnoclines with parametrization as described in text.

The emphasis of this paper is on the perturbation theory applied to a physical problem that was motivated by numerical calculations. The companion paper by Weidman & Johnson (1982) shows the predicted leapfrogging solitary waves experimentally, with reasonable quantitative agreement except for the additional influence of viscous damping.

2. Analysis

Three homogeneous fluid layers of thickness H_1, H_2 and H_3 are separated by two thin layers of thickness $2h_1$ and $2h_2$ with gradually changing densities as shown schematically in figure 1. The analysis of Liu *et al.* (1980) leads to two coupled equations for the evolution of the wave amplitudes $A(\xi, T)$ and $B(\xi, T)$ of single-mode, weakly nonlinear, long internal waves, each in one pycnocline:

$$A_T + \alpha_1 A A_\xi - \beta_1 \frac{\partial^2}{\partial \xi^2} \mathscr{H}_1(A) - \beta_1 \frac{\partial^2}{\partial \xi_2} \mathscr{H}_2(B) = 0, \tag{1a}$$

$$B_T - \Delta C B_\xi + \alpha_2 B B_\xi - \beta_2 \frac{\partial^2}{\partial \xi^2} \mathscr{H}_3(B) - \beta_2 \frac{\partial^2}{\partial \xi^2} \mathscr{H}_2(A) = 0, \tag{1b}$$

where the operator $\mathscr{H}_1$ is

$$\mathscr{H}_1(A) = \frac{1}{2H_1} \int_{-\infty}^{\infty} A(\xi', T) \coth \frac{\pi(\xi - \xi')}{2H_1} d\xi' + \frac{1}{2H_2} \int_{-\infty}^{\infty} A(\xi', T) \coth \frac{\pi(\xi - \xi')}{2H_2} d\xi'. \tag{2}$$

The operator $\mathscr{H}_3$ for the bottom pycnocline depth equals $\mathscr{H}_1$ with H_1 replaced by H_3.

Wave B is coupled to wave A through the operator

$$\mathscr{H}_2(B) = \frac{1}{2H_2} \int_{-\infty}^{\infty} B(\xi', T) \tanh \frac{\pi(\xi - \xi')}{2H_2} d\xi'. \tag{3}$$

The interaction is proportional to the wave amplitude in the other pycnocline, and decreases with increasing interpycnocline distance H_2.

The time T and space variable ξ are in a reference frame moving with the upper linear wave speed C_0. α and β are environmental parameters that measure the strength of nonlinearity and dispersion in each pycnocline separately; ΔC is the difference between the upper and lower linear wave speeds.

For a mode-two solitary internal wave in a finite-depth fluid with a single pycnocline located in the middle of the tank, $H_1 = H_2 \equiv H$, the steady-state wave-amplitude solution is (Joseph 1977)

$$A(\xi) = 2A_m \left[\cos\delta_1 + \cosh\left(\frac{\xi\delta_1}{H}\right)\right]^{-1}, \tag{4a}$$

where the parameter of non-dimensional width δ_1 determines the maximum amplitude

$$A_0 = \frac{2A_m}{1+\cos\delta_1} = \frac{4\beta_1\delta_1\tan\frac{1}{2}\delta_1}{\alpha_1 H}. \tag{4b}$$

Joseph's solution is the natural connection between the Benjamin–Ono deep-water ($\delta_1 \to \pi$) and Korteweg–de Vries shallow-water ($\delta_1 \to 0$) solutions (Henyey 1980). Equation (4) is rigorously true only when a single pycnocline is halfway between the top and bottom of the wave tank; however, when the supporting pycnocline is not exactly halfway, or in the presence of a second distant pycnocline, the stationary wave shape is well approximated by (4) if $|H_1 - H_2|/(H_1 + H_2) \ll 1$ (Liu *et al.* 1980). Hence, in the rest of this analysis we use Joseph's solution.

In the absence of coupling between pycnoclines, the energy of individual waves is conserved. With coupling included, the energy changes according to

$$\frac{d}{dt}\left[\frac{1}{2\beta_1}\int_{-\infty}^{\infty} A^2 d\xi\right] = \int_{-\infty}^{\infty} A\,\frac{\partial^2}{\partial\xi^2}\mathscr{H}_2(B)\,d\xi. \tag{5}$$

Similarly, the energy of wave B satisfies

$$\frac{d}{dt}\left[\frac{1}{2\beta_2}\int_{-\infty}^{\infty} B^2 d\xi\right] = \int_{-\infty}^{\infty} B\,\frac{\partial^2}{\partial\xi^2}\mathscr{H}_2(A)\,d\xi. \tag{6}$$

However, even though the energy of the individual waves is not conserved in general, the total energy of the combined system is conserved.

For large separation distances between two pycnoclines, there is a small non-dimensional parameter for the interaction, $\Delta \equiv (\lambda/H)^2$, where λ is the characteristic wavelength. In this case, the problem possesses three distinct timescales: the time-scale for wave motion, λ/C_0; for wave evolution, λ^2/hC_0; and for wave-amplitude oscillation, H^2/hC_0. When $\Delta \ll 1$, the coupling term is small compared with the non-linear and dispersive terms, and so the coupling is weak.

For weak coupling it is usually a good approximation to assume that the shape of the solitary wave – a reflection of the balance between nonlinearity and dispersion – does not change, but that the soliton parameters change in accordance with the energy loss. The result is an ordinary differential equation for the parameter δ_1 of the first wave, coupled to a similar equation for the parameter δ_2 of the second wave. These equations involve the horizontal separation $\theta(t)$ between the upper wave and the lower wave, defined implicitly in the expression for the wave amplitude of the lower wave:

$$B(\xi) = 2B_m \left[\cos\delta_2 + \cosh\left(\frac{\delta_2(\xi-\theta)}{H}\right)\right]^{-1}. \tag{7}$$

The lower solitary wave is found ahead of the upper solitary wave for $\theta > 0$.

The wave energy of wave A in terms of δ_1 is

$$\frac{1}{2\beta_1}\int_{-\infty}^{\infty} A^2 d\xi = \frac{16\pi^2\beta_1\delta_1}{\alpha_1^2 H}\{1-\delta_1\cot\delta_1\}. \tag{8}$$

By using Parseval's theorem and the Fourier transform, the coupling term becomes

$$\int_{-\infty}^{\infty} A\frac{\partial^2}{\partial\xi^2}\mathscr{H}_2(B)\,d\xi = \frac{32\pi^3\beta_1\beta_2}{\alpha_1\alpha_2 H^3} I(\delta_1,\delta_2,\theta), \tag{9a}$$

with

$$I(\delta_1,\delta_2,\theta) = \int_{-\infty}^{\infty}\frac{K^2\sinh K\sin(K\theta/H)\,dK}{\sinh(\pi K/\delta_1)\sinh(\pi K/\delta_2)}. \tag{9b}$$

The final set of equations for the wave paramteers δ_1 and δ_2 is then

$$\frac{d\delta_1}{dt} = \frac{2\pi\beta_2\alpha_1}{\alpha_2 H^2}F(\delta_1)\,I(\delta_1,\delta_2,\theta), \tag{10a}$$

$$\frac{d\delta_2}{dt} = -\frac{2\pi\beta_1\alpha_2}{\alpha_1 H^2}F(\delta_2)\,I(\delta_1,\delta_2,\theta). \tag{10b}$$

The function $F(\delta)$ is the inverse of the derivative of the wave energy (8) with respect to the parameter δ:

$$\left(\frac{dE}{d\delta}\right)^{-1} = F(\delta) = \frac{\sin^2\delta}{(\delta\sin\delta)^2+(\sin\delta-\delta\cos\delta)^2}, \tag{11}$$

which is always positive, because the wave energy increases with δ.

Equations (10a, b) are supplemented by an equation for the wave separation θ, whose time derivative is the difference between the individual wave speeds

$$\frac{d\theta}{dt} = \Delta C - \frac{2}{H}[\beta_1(\delta_1\cot\delta_1-1)-\beta_2(\delta_2\cot\delta_2-1)]. \tag{12}$$

It is clear from (9b) that the interaction vanishes when the horizontal separation θ between waves is zero. Such waves constitute a stationary state when their speeds are equal. On the other hand, for large separation θ, the integrand in (9b) is oscillatory, and $I(\delta_1,\delta_2,\theta)$ approaches zero. Therefore widely separated waves do not interact, and propagate with no change in shape.

Although much simpler than the original partial differential equations, the ordinary differential equations (10a, b) and (12) for δ_1, δ_2 and θ are still too complicated for analytical study to gain some physical insight, but small oscillations can be treated analytically.

The equilibrium state has one wave in each pycnocline with equal speeds and no horizontal separation. The wave parameters at equilibrium, δ_{10} and δ_{20}, are related by the equal-speed condition

$$\beta_1(\delta_{10}\cot\delta_{10}-1) = \beta_2(\delta_{20}\cot\delta_{20}-1)+\tfrac{1}{2}H\Delta C. \tag{13}$$

Small oscillations about the equilibrium are obtained by putting $\delta_1(t) = \delta_{10}+\Delta_1(t)$ and $\delta_2(t) = \delta_{20}+\Delta_2(t)$, where the Δs are assumed to be small. The relation between the oscillation amplitudes Δ_1 and Δ_2, from (10a, b), is

$$\frac{d\Delta_2}{dt} = -\frac{\beta_1}{\beta_2}\frac{\alpha_2^2}{\alpha_1^2}\frac{F(\delta_{20})}{F(\delta_{10})}\frac{d\Delta_1}{dt}. \tag{14}$$

Small oscillations around the equilibrium state also imply that the relative position θ of the waves remains small compared with a characteristic length. In this case the interaction term becomes linear in θ:

$$I(\delta_{20}, \delta_{10}, \theta) = \frac{\theta}{H}\int_{-\infty}^{\infty} \frac{K^3 \sinh K\, dK}{\sinh(\pi K/\delta_{10}) \sinh(\pi K/\delta_{20})}. \tag{15}$$

This is justified because the integral is cut off at $K \simeq \max(\delta_{10}, \delta_{20})$. With these approximations, the three ordinary differential equations (10*a*, *b*) and (12) coalesce into the simple-harmonic-oscillation equation

$$d^2\Delta_1/dt^2 = -\omega^2(\delta_{10}, \delta_{20})\,\Delta_1, \tag{16}$$

where the frequency $\omega(\delta_{10}, \delta_{20})$ is a complicated function involving (15).

In order to interpret the frequency physically, (15) is still too complicated; the final restriction is that the wave widths at equilibrium, δ_{10} and δ_{20}, are comparable. This assumption allows the evaluation of the integrand at an appropriately defined intermediate value δ_0 between δ_{10} and δ_{20}. A natural value for δ_0 is

$$\delta_0 = \tfrac{1}{2}(\delta_{10} + \delta_{20}). \tag{17}$$

With this intermediate δ_0 the expression for the frequency $\omega = \omega(\delta_0)$ is

$$\omega^2 = \frac{2\beta_1\beta_2}{\alpha_1\alpha_2 H^4}(\alpha_1^2 + \alpha_2^2)\, F(\delta_0)\, G(\delta_0)\, J(\delta_0). \tag{18}$$

Here, F is given by (11), and G is defined by

$$G(\delta_0) \equiv 2\pi\int_{-\infty}^{\infty} \frac{K^3 \sinh K\, dK}{\sinh^2(k\pi/\delta_0)} = \frac{\delta_0 - 3\sin\delta_0 + 2\delta_0\cos^2\frac{1}{2}\delta_0}{2\sin^4\frac{1}{2}\delta_0}\,\delta_0^4. \tag{19}$$

$J(\delta_0)$ is the derivative of the wave speed with respect to the width δ_0:

$$J(\delta_0) = (\delta_0 - \tfrac{1}{2}\sin 2\delta_0)/\sin^2\delta_0. \tag{20}$$

The dependence of the frequency on δ_0 is contained in the complicated function FGJ, which is plotted in figure 2. In general, the large separation distance has a weak influence on the soliton shape (through the width δ), which, in turn, has a weak influence on the function $F(\delta)\,G(\delta)\,J(\delta)$. Therefore, in order to simplify the results further for application purposes, we take the limit $\delta_0 \to \pi$ (Benjamin–Ono soliton) while keeping H large but fixed and neglecting the linear wave-speed difference ΔC. In this limit the product FJ approaches π^{-1}, and G approaches $\frac{1}{2}\pi^5$. Thus the frequency of small oscillations for a Benjamin–Ono soliton reduces to

$$\omega = \frac{3\pi^2}{8}\frac{C_0}{H}\frac{(h_1^2 + h_2^2)^{\frac{1}{2}}}{H}. \tag{21}$$

This result is expressed in the physical parameters; the linear wave speed C_0, pycnocline thicknesses h_1 and h_2, and separation distance H. It is to be noted that the period of oscillation $2\pi/\omega$ is indeed much larger than the period of wave motion and also larger than the timescale for the evolution of the solitary wave, as indicated before. Equations (18) and (21) are used for comparison with the wave-tank experiments described in the companion paper by Weidman & Johnson (1982).

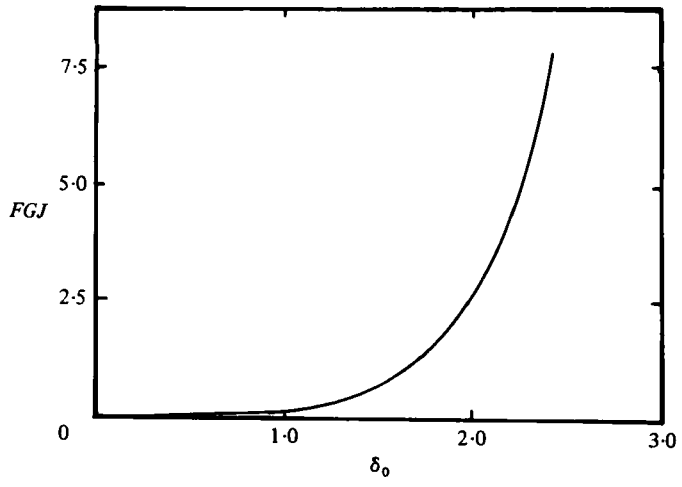

FIGURE 2. The frequency coefficient FGJ as a function of soliton parameter δ_0.

3. Results and discussion

The analytical expression for the frequency of small oscillations in (18) involves many approximations, but they are not essential. These approximations are made only because the coefficients that occur in the ordinary differential equations (10*a*, *b*) are too complicated for analytical evaluation. Therefore, it is interesting to compare the numerical results of (10*a*, *b*) and (12) with the analytical estimates from (18).

In order to make comparisons with the results of Liu *et al.* (1980), we take their pycnocline parameters α and β as $\alpha = 6C_0/5h$ and $\beta = \frac{3}{8}hC_0$ for the hyperbolic-tangent density profile. There the linear wave speed is $C_0 = 3{\cdot}87$ and h is the pycnocline thickness; $h = 1$ for the upper and $h = 1{\cdot}4$ for the lower pycnocline. The numerical values for these parameters are typical of a laboratory experiment in which the units of length are centimetres and the units of time are seconds. Before assessing the influence of the parameters on the oscillation period, we compute one particular case from (10*a*, *b*) and (12) with $H = 10$, $\delta_{10} = 1{\cdot}84$, $\delta_{20} = 1{\cdot}62$ and the maximum separation $\theta_m = 8$, as shown in figure 3. It is clear that this result (the dashed line) is very similar to the result of Liu *et al.* (1980) (the solid line) apart from a difference in the initial time to accommodate the initial transients. It is to be noted that the amplitudes A_0 and B_0 and the separation θ are perfectly periodic, albeit not exactly sinusoidal, and both results agree quantitatively with less than 15 % difference of the oscillation periods.

For small θ_m, the numerically computed period T_e from (10*a*, *b*) and (12), and the theoretical period T_{th} from (18) agree well, as shown in figure 4(*a*) for $\theta_m = 8$. It is to be noted that the period T of wave-amplitude oscillation increases as H^2 for large H. Figure 4(*b*) shows the period as a function of the maximum separation θ_m. The theoretical value T_{th} is close to the limit $\theta \to 0$, and the period T increases roughly exponentially for large θ. From figure 4(*b*), there appears to be a maximum relative position of waves beyond which there is no oscillatory behaviour. In general, the results from the small-oscillation approximation compare reasonably well with the numerical results obtained from (10*a*, *b*) and (12).

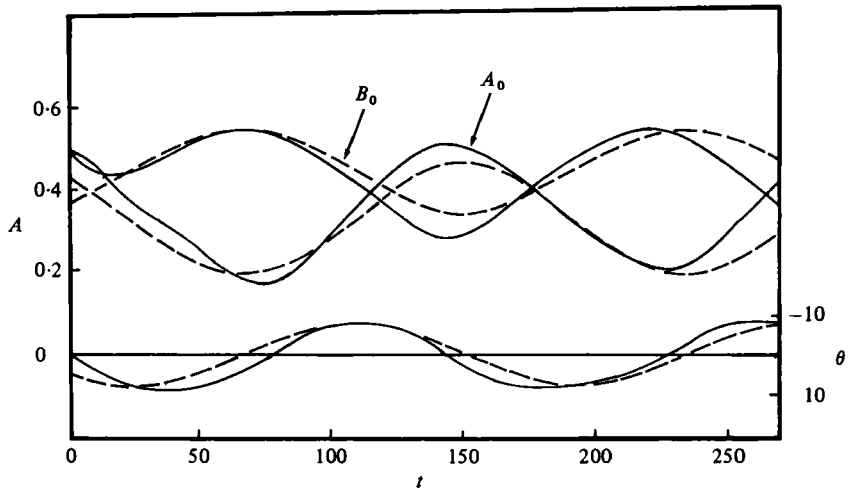

FIGURE 3. Comparison of the amplitude and phase of two leapfrogging solitons computed numerically from (10*a*, *b*) and (12) (the dashed line) with the results of Liu *et al.* (1980) (the solid line); $H = 10$, $\delta_{01} = 1{\cdot}92$, $\delta_{02} = 1{\cdot}70$, $\theta_m = 8$, $\Delta C = 0$.

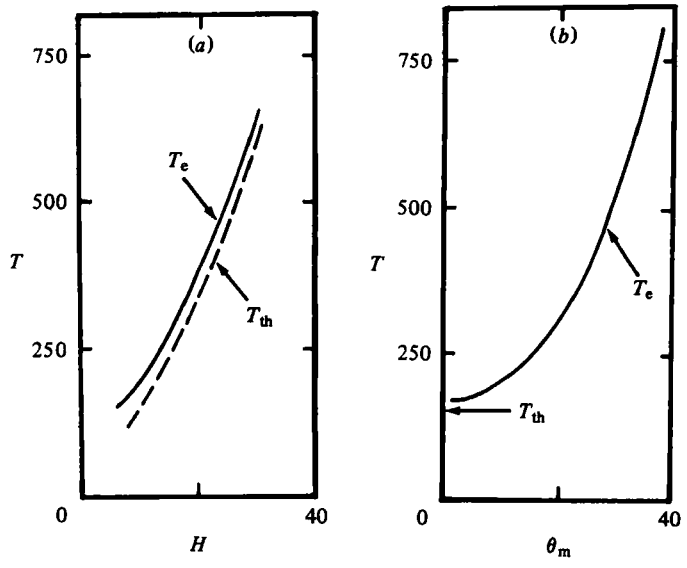

FIGURE 4. Comparison between theoretical period T_{th} defined by (18), and the numerical value T_e computed from (10*a*, *b*) and (12). (*a*) Oscillation period as function of pycnocline separation distance H; $\theta_m = 8$, $\Delta C = 0$. (*b*) Numerical oscillation period T_e as function of maximum soliton distance θ_m; $H = 10$, $\delta_{01} = 1{\cdot}84$, $\delta_{02} = 1{\cdot}62$, $\Delta C = 0$.

4. Concluding remarks

This study considers solitary waves on two distinct but neighbouring pycnoclines with thicknesses much smaller than a characteristic wavelength. Each solitary wave maintains the relation between amplitude, width and velocity, but slowly changes these parameters to comply with the effect of energy exchange. Three ordinary differential equations describe the widths and the horizontal separation of the solitary

waves. A simple formula is obtained for the oscillation frequency about the equilibrium. The results agree quantitatively with previous numerical computations by Liu *et al.* (1980), except for the initial transients, and with the subsequent experiment by Weidman & Johnson (1982), except for viscous damping.

This work was partially supported by APL/JHU Subcontract no. 600575 to Dynamics Technology Inc. One of the authors (N. R. P.) acknowledges the hospitality of the Aerospace Engineering Department at the University of Southern California, where part of his work was performed. Our discussions with P. Weidman have contributed substantially to this paper.

REFERENCES

BENJAMIN, T. B. 1966 Internal waves of finite amplitude and permanent form. *J. Fluid Mech.* **25**, 241–270.

BENJAMIN, T. B. 1967 Internal waves of permanent form in fluids of great depth. *J. Fluid Mech.* **29**, 559–592.

BENNEY, D. J. 1966 Long non-linear waves in fluid flows. *J. Math. & Phys.* **45**, 52–63.

ECKART, C. 1961 Internal waves in the ocean. *Phys. Fluids* **4**, 791–799.

HENYEY, F. S. 1980 Finite-depth and infinite-depth internal-wave solitons. *Phys. Rev.* A **21**, 1054–1056.

JOSEPH, R. I. 1977 Solitary waves in a finite depth fluid. *J. Phys.* A: *Math. Gen.* **10**, L225–L226.

KEULEGAN, G. H. 1953 Characteristics of internal solitary waves. *J. Res. Nat. Bur. Stand.* **51**, 133–140.

KUBOTA, T., KO, D. R. S. & DOBBS, L. 1978 Propagation of weakly nonlinear internal waves in a stratified fluid of finite depth. *J. Hydronautics* **12**, 157–165.

LIU, A. K., KUBOTA, T. & KO, D. R. S. 1980 Resonant transfer of energy between nonlinear waves in neighbouring pycnoclines. *Stud. Appl. Math.* **63**, 25–45.

LONG, R. R. 1956 Solitary waves in the one and two fluid systems. *Tellus* **8**, 460–471.

ONO, H. 1975 Algebraic solitary waves in stratified fluids. *J. Phys. Soc. Japan* **39**, 1082–1091.

PEREIRA, N. R. & REDEKOPP, L. G. 1980 Radiation damping of long, finite amplitude internal waves. *Phys. Fluids* **23**, 2182–2183.

WEIDMAN, P. D. & JOHNSON, M. 1982 Experiments on leapfrogging internal solitary waves. *J. Fluid Mech.* **122**, 195–213.